Effect of thrust coefficient on the flow blockage effects in closely-spaced spanwise-infinite turbine arrays

Effect of thrust coefficient on the flow blockage effects in closely-spaced spanwise-infinite turbine arrays

Jessica M. I. Strickland and Richard J. A. M. Stevens

Physics of Fluids Group, Max Planck Center Twente for Complex Fluid Dynamics, J. M. Burgers Center for Fluid Dynamics, and MESA+ Research Institute, University of Twente, P.O. Box 217, 7500 AE Enschede, The Netherlands

E-mail: j.strickland@utwente.nl

Abstract. The performance of a wind turbine within an array is not necessarily equivalent to the performance of a free-standing turbine because the presence of the neighboring turbines influences the incoming flow. However, insight into these blockage effects is still lacking. Here, we use large eddy simulations to investigate how the blockage effect depends on the turbine thrust coefficient C_T. We consider three main scenarios: a free-standing turbine, a closely-spaced spanwise-infinite row of turbines, and an entire wind farm with a high turbine density. We observe that the power production of turbines in the row increases approximately linearly with C_T' when compared to the production of a free-standing turbine. Here, $C_T' = C_T/(1-a)^2$ where a is the induction factor. In contrast, the power output of turbines in the first row of a wind farm decreases approximately linearly with C_T when compared to the production of turbines in a corresponding, solitary row.

1. Introduction

Accurately modeling wind farm performance is becoming more important as global energy demands and investments in wind energy grow at an unprecedented rate [1, 2]. The main goal of most wind farm models is to obtain accurate turbine power production estimates. Currently, most models focus on the physics downstream of the turbines. For instance, wind turbine wake models typically impose wake deficits downstream to reflect the extracted kinetic energy [1]. As modeling wake effects and wake interactions in large wind farms is still quite challenging, it is still common practice to normalize the power production of downstream turbine rows with the power production of the first row. By normalizing data using the first row, it is implicitly assumed that the first row is always performing as it would in isolation without downstream turbines.

Although this assumption is appealing, it is not correct. Downstream turbines can influence upstream turbines as it follows from actuator disk theory that the flow upstream of a turbine is affected by its presence [3]. Due to blockage effects, the performance of a turbine in the first row of a wind farm is not necessarily equal to that of a turbine placed in isolation. Given that the power output of the first turbine row is often used as a reference, accounting for blockage effects and understanding the relevant parameters is crucial to arrive at reliable estimates for the power production of large wind farms.

Previous studies have shown that blockage can both increase and decrease the power output of neighboring turbines and have highlighted the importance of understanding the effects for a

wider range of conditions [4–10]. Previous experiments and simulations [5, 8] have shown that the power output of laterally closely-spaced turbines can be higher than that of isolated turbines. This increase is due to a Venturi effect, i.e., the flow is accelerated between the closely-spaced turbines causing their power output to increase significantly. The increased power production is essentially a blockage or confinement effect due to which additional wind is forced through the turbine swept area.

For large wind farms another effect is observed. Segalini and Dahlberg [9] and Bleeg et al. [4] namely show that for large wind farms, the flow velocity at the first row can be significantly reduced as the wind is deflected over and around the entire wind farm. As a result, turbines in the first row will produce less energy than they would without the downstream turbines being present. In this study, we use large eddy simulations to better understand the effect of the turbine thrust coefficient on the flow blockage effect and to ultimately provide more accurate predictions of its impact on the wind farm performance.

This paper is divided into three main sections to follow. Section 2 describes the modeling details and case parameters and characteristics. Next, the results are presented in Section 3, addressing the dependence of the blockage effect on the thrust coefficient. Finally, the major conclusions are summarized in Section 4.

2. Numerical set-up

Here we outline the numerical framework of the large eddy simulations (LES) followed by the specific cases and parameters examined.

2.1. Large eddy simulations model

Our large eddy simulations for neutral atmospheric boundary layers (ABL) are governed by the filtered incompressible Navier-Stokes equations without buoyancy, system rotation, or other effects,

$$\partial_t \tilde{u}_t + \partial_j(\tilde{u}_i\tilde{u}_j) = -\partial_i\tilde{p}^* - \partial_j\tau_{ij} - \delta_{i1}\partial_1 p_\infty/\rho + f_i \tag{1}$$

$$\partial_i\tilde{u}_i = 0 \tag{2}$$

where $\tilde{u}$ is the filtered velocity field and $\tilde{p}^*$ is the filtered modified pressure such that $\tilde{p}^* = \tilde{p}/\rho + \tau_{kk}/3 - p_\infty/\rho$. The sub-grid scale stresses are represented in the term τ_{ij}. The deviatoric part, $\tau_{ij} - \delta_{ij}\tau_{kk}/3$, is parametrized using a eddy-viscosity sub-grid scale model. Specifically, we employ the Lagrangian scale-dependent dynamic sub-grid model and the latter term ($\delta_{ij}\tau_{kk}/3$) is combined into the modified pressure. The turbine forcing is represented by f_i and the viscous forces are neglected as we consider high Reynolds number atmospheric flows.

The governing equations are solved as follows. The time integration is performed using a second-order accurate Adams-Bashforth scheme. We consider periodic boundary conditions in the horizontal directions, as a pseudo-spectral discretization is used. The top boundary is characterized by a no-stress condition with the vertical velocity set to zero. The stress at the bottom boundary is related to the velocity of the first grid point relying on the classic logarithmic law for turbulent wall-bounded flow [11, 12]. In our cases the surface roughness characterizing the logarithmic law is set to a typical offshore value: $z_0 = 0.001$ m [13].

A concurrent precursor method is used to generate realistic ABL inflow conditions. Two domains are considered simultaneously: a fully developed neutral ABL which is used to create realistic inflow for a second domain that contains wind turbines. The turbulent inflow data is sampled from the ABL simulation and is introduced at the entrance of the target wind farm domain via a fringe region. Further details about the simulation approach can be found in Ref. [14].

The actuator disk model is used to represent the turbines [14–16]. This method incorporates the turbines as disks that exert a total thrust force

$$F_t = -\frac{1}{2}\rho C_T U_\infty^2 A \tag{3}$$

where ρ is the density of air, $A = \frac{\pi}{4}D^2$ is the area of the rotor disk, and C_T is the thrust coefficient. Equation 3 requires the undisturbed upstream velocity U_∞. However, identifying the upstream velocity can be difficult in wind farm simulations. To circumvent this issue, the use of the velocity at the turbine location is preferred [15,17]. This is achieved by using actuator disk theory to relate the velocity across the disk U_D with the thrust coefficient C_T' which is defined as per the following relationship

$$C_T' = \frac{C_T}{(1-a)^2}, \text{ where } a = \frac{U_\infty - U_D}{U_\infty} \tag{4}$$

where a is the axial induction factor which relates the velocity across the disk to the velocity upstream and $C_T = 4a(1-a)$ [18]. In our simulations, each turbine is assigned the same C_T'. This simplification is based on a reasonable assumption that the turbines will mostly operate in a regime where the thrust coefficient will be independent of wind speed [19]. Though the actuator disk model is not an exact representation of the turbines, this method is widely used in the literature and provides useful insight when the thrust coefficient is lower than the Betz limit ($C_T = 8/9, a = 1/3$, $C_T' = 2$). By multiplying the drag force by the average velocity across the disk, we obtain an expression for the power produced by the turbines: $P = -F_t U_D$. Therefore, we calculate the power output of the turbines using the following expression.

$$P = \frac{1}{2}\rho C_T' {U_D}^3 \frac{\pi}{4} D^2 \tag{5}$$

Additionally, in our analysis we consider time-averaged values. We perform simulations for a sufficient period to ensure that the wind farm data is converged. Time-averaging begins after 20 dimensionless time units (approximately 40 flow-through times) when the statistical stationary state is reached. The error bars are calculated using the standard deviation of the average power obtained from successive intervals of 20 time units after the start of time-averaging and following the general rules for the propagation of uncertainties. Also, we normalize the turbine power output for each simulation with the incoming flow at hub-height to accurately compare the performance data from different simulations.

2.2. Simulation specifications

We study three main layouts as illustrated in Figure 1 and the details of the simulations are summarized in Table 1. First, to investigate flow blockage effects in laterally closely-spaced rows, we compare the performance of turbines in an infinite row to that of a free-standing turbine. Then, we investigate the effect of turbines placed downstream by comparing the front row of a dense, spanwise-infinite, wind farm with eight rows in the downstream direction, to that of a solitary row with the same spanwise turbine spacing. Though the dimensionless streamwise (s_x) and spanwise (s_y) turbine spacing are also varied, we primarily focus on the dependence of the blockage effect on the turbine thrust coefficient in the current analysis.

For all cases we consider the following fixed parameters. Both the turbine hub-height (z_h) and diameter (D) are 100 m. The non-dimensional domain size used is $L_x, L_y, L_z = (4\pi, \pi, 1.0)$, which is discretized on a grid with $N_x, N_y, N_z = (512, 128, 128)$ nodes in the streamwise, spanwise, and vertical direction, respectively. The domain size is made dimensionless using the height of the domain H. The streamwise location of the (first) row of turbines is constant, $x/H = 5.0$, to ensure there is ample space preceding the farm to observe the upstream influence

of the wind turbines. Unless otherwise mentioned, $H = 1000$ m, which is a typical height for a neutral ABL [15].

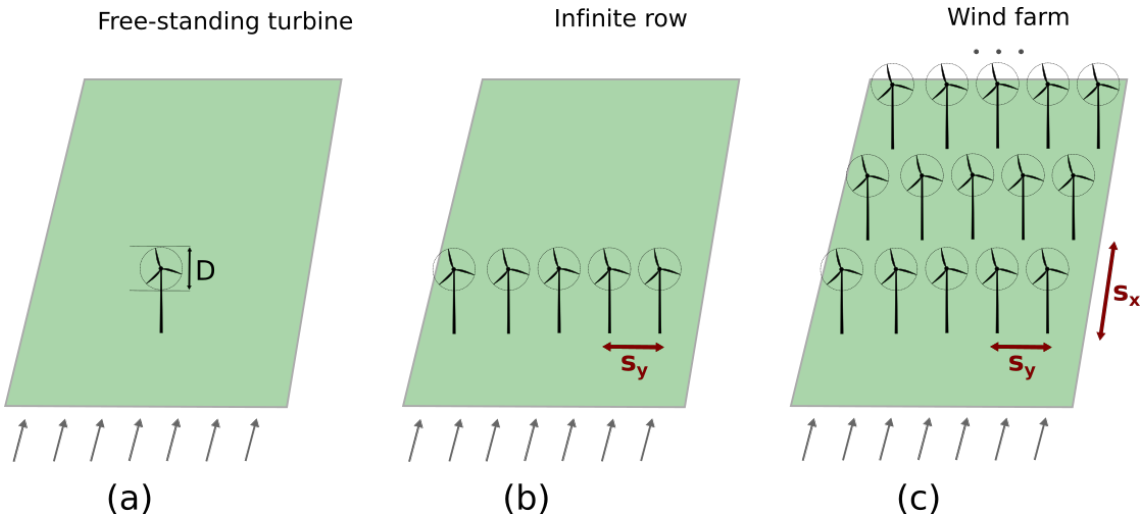

Figure 1. Schematic depicting the three main cases considered in this study: (a) a free-standing turbine (b) an infinite row, and (c) a wind farm with eight rows in the downstream direction. The streamwise (s_x) and spanwise (s_y) spacing are made non-dimensional using the turbine diameter D, i.e., $s_x = S_x/D$, $s_y = S_y/D$. See Table 1 for a detailed overview of the cases considered.

Table 1. Summary of the simulated cases. The variables of interest are the non-dimensional streamwise (s_x) and spanwise (s_y) spacing, and the thrust coefficient (C_T'), see Equation 4.

Case	s_y	s_x	C_T'
Wind farm (8 rows)	1.57	1.96, 3.93, 7.85	1/6, 1/3, 2/3, 1, 4/3, 5/3
Infinite row	1.26, 1.57	-	1/3, 2/3, 1, 4/3, 5/3
Free-standing turbine	-	-	1/3, 2/3, 1, 4/3, 5/3

3. Results

Here we examine the impact of the turbine thrust coefficient on the blockage effect. First, we compare the power output of a turbine in a closely-spaced spanwise-infinite row to that of a free-standing turbine. Next, the performance of the front row of a wind farm is compared to both the corresponding row case and a free-standing turbine.

3.1. Blockage effects for an infinite row of turbines

Figure 2 shows the relative power output of the average turbine in a closely-spaced, laterally-infinite row compared to a free-standing turbine. The figure shows that blockage can significantly increase the power production of turbines in an infinite row. Our simulation results are in agreement with previous experimental observations by McTavish et al. [7, 8], who showed that flow blockage can increase the turbine power production by 3% to 9% for $1 \leq s_y \leq 2$. Here, the

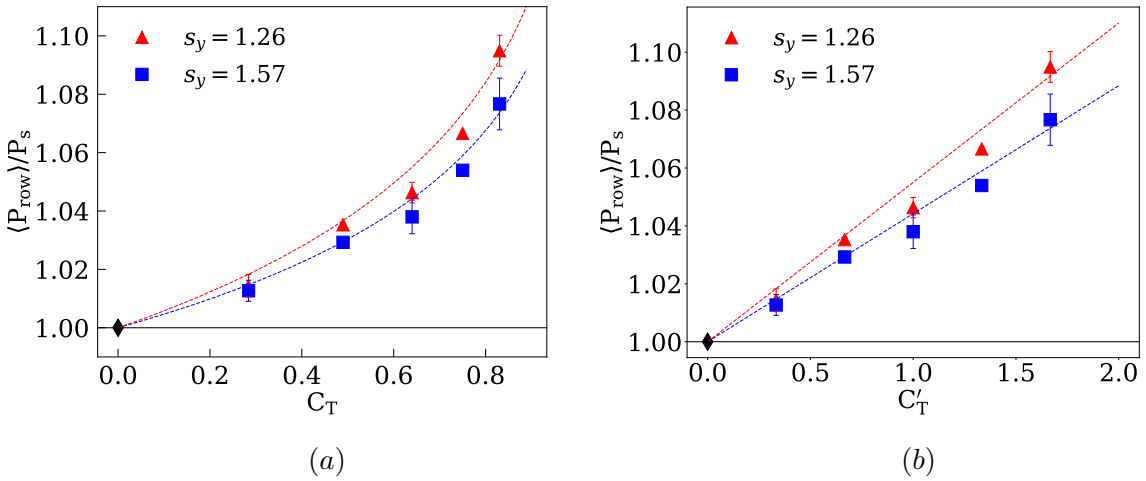

Figure 2. The average power output of a turbine in an infinite, closely-spaced (s_y) row relative to the average power output of a free-standing turbine as a function of a) C_T and b) C'_T. The dashed lines indicate the least-squares fit to the $\langle P_{row} \rangle / P_s$ versus C'_T data in the right figure. The corresponding lines in the left figure are obtained using Equation 4.

main effect is the speed-up of the flow between the closely-spaced turbines. Due to this Venturi effect, the power output of the turbines in the array increases compared to the power output of an isolated turbine. The observed effect is more prominent for the $s_y = 1.26$ row compared to the less dense, $s_y = 1.57$ case. Furthermore, we observe that the relative power output increases approximately linearly with C'_T.

It is important to consider that the domain height may influence this result. As the turbines are located relatively close to the ground, the wind cannot accelerate under the wind turbines. This means that the air is essentially limited to flow through or over the wind turbine array. However, the height of the ABL may limit the flow acceleration above the wind farm. We selected a domain height $H = 1000$ m because it is a typical height for a neutral ABL [15]. To test the potential effect of vertical confinement, we increased the domain height. We find that for $C'_T = 5/3$, $s_y = 1.26$, the average power output of a turbine in an infinite row compared to that of a free-standing turbine is only 0.9% lower when the domain height is increased from $H = 1000$ m to 2000 m. Regardless, we emphasize that for realistic atmospheric conditions, the capping inversion limits the ABL height from several hundred meters to about 1000 m.

3.2. Blockage effects for a wind farm

Here, we analyze the performance of the front row of different wind farm layouts to address how placing additional rows downstream affects the performance of the turbines in the first row. We observed that the blockage effect increases linearly with C'_T for an infinite row when compared to a free-standing turbine. However, placing turbines downstream also introduces a blockage effect. Figure 3 shows the average power output of a turbine in the front row of a wind farm compared to the average power output of a turbine within a corresponding, solitary row for various thrust coefficients and streamwise spacings. The figure shows that the average power production of the turbines in the first row of each wind farm is lower than the corresponding isolated row and decreases approximately linearly with C_T. This behavior is due to the presence of the downstream turbines which force more of the flow to go over the wind farm, lowering the velocity at hub-height at the entrance of the wind farm. Therefore, we find that the blockage effect is more pronounced when the streamwise spacing is smaller, i.e., for

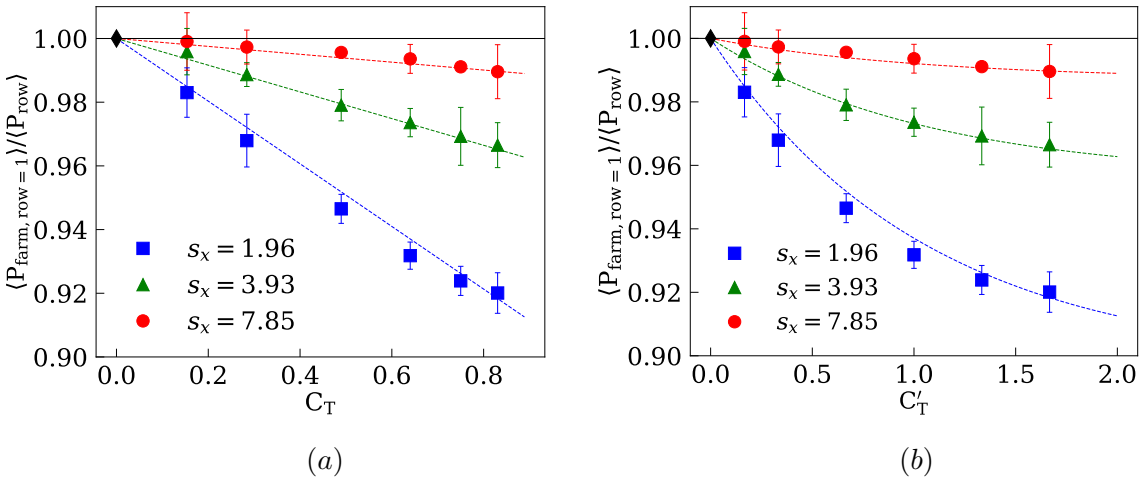

Figure 3. The power output for the average turbine in the first row of a wind farm with $s_y = 1.57$ and different streamwise spacings (s_x) is compared to that of a solitary, infinite row as a function of a) C_T and b) C'_T. The dashed lines indicate the least-squares fit to the $\langle P_{farm,row=1}\rangle/\langle P_{row}\rangle$ versus C_T data in the left figure. The corresponding lines in the right figure are obtained using Equation 4.

denser wind farms. Though we compare different layouts, the same linear dependence was also observed by Segalini and Dahlberg; however, we do not observe that this global effect saturates at high C_T as they did [9]. Besides, we note that this global blockage effect contrasts the blockage effect observed in the previous section which depends linearly on C'_T, emphasizing that different physical mechanisms play a role.

In Figure 4, we compare the relative performance of the average turbine in the front row of a wind farm to a free-standing turbine as a function of the thrust coefficient. Here, we observe the effect of the two types of blockage that we have already established. First, the beneficial effect of close lateral spacing is present, where the average power output of a turbine in an infinite row relative to a free-standing turbine increases approximately linearly with C'_T. Second, the effect of downstream, closely-spaced turbines was shown to reduce the performance of the front row linearly with C_T. The results in Figure 4 suggest that the relative performance of the front row of a wind farm compared to a free-standing turbine depends on the thrust coefficient but without a universal relationship. For $s_x = 1.96$, the average turbine in the first row produces less power than a free-standing turbine for each thrust coefficient. The layouts with a lower turbine density ($s_x = 3.93, 7.85$) exhibit an overall relative benefit from the blockage. This contrasts the results by Bleeg et al. [4], who showed that the performance of the first row decreases compared to an isolated reference turbine. However, we note that we are considering a spanwise-infinite wind farm, which does not allow flow around the wind farm, and this could enhance the observed blockage effects in our case.

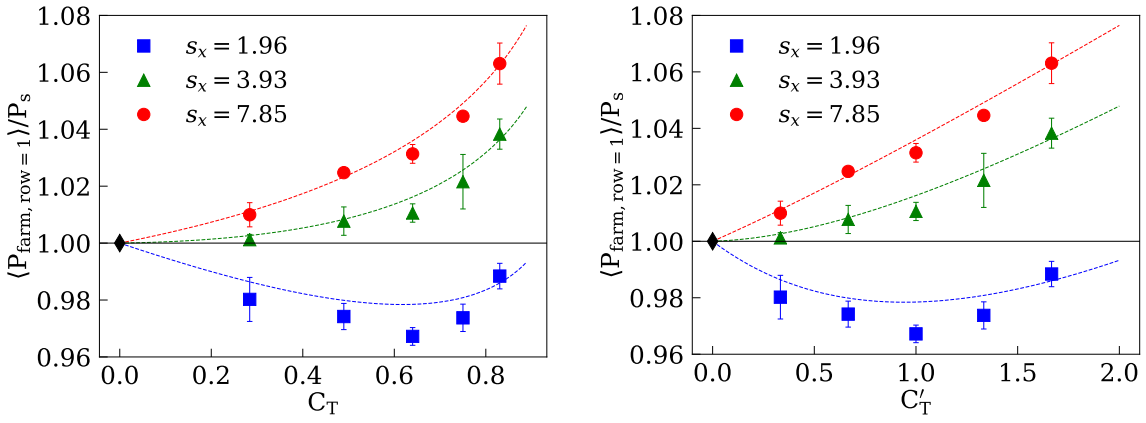

Figure 4. The power output for the average turbine in the first row of a wind farm with $s_y = 1.57$ and different streamwise spacings (s_x) is compared to that of a free-standing turbine as a function of a) C_T and b) C'_T. The dashed lines are calculated from the fits obtained in Figures 2 and 3.

4. Conclusions

We used large eddy simulations to study the impact of the turbine thrust coefficient on the blockage effect. We compared the performance of the front row of a tightly packed wind farm, a solitary infinite turbine row, and a free-standing turbine. Overall, we have shown that the blockage effect is enhanced as the thrust coefficient increases. First of all, the average turbine in a closely-spaced infinite row produces more power than a free-standing turbine and the relative power output increases approximately linearly with C'_T. This relative benefit in performance was also observed by others using both models and experiments [5–8]. We acknowledge that the observed performance enhancement may be more pronounced than in real wind farms because we consider spanwise-infinite arrays in which the flow cannot go around the wind farm [4]. Secondly, we observed that the average turbine in the front row of a wind farm produces less power than a turbine within the corresponding solitary row. In agreement with the results of Segalini and Dahlberg [9], we find that this blockage effect is approximately linear with C_T. Ultimately, our results show that the power output of a turbine depends on the layout of the wind farm as well as the turbine thrust coefficient. Future work should investigate the effect of the wind farm layout (different combinations of s_x and s_y) and the effect of the lateral confinement on these blockage effects.

Acknowledgements: We would like to acknowledge the assistance of Gijs Hannink, BSc. for his contributions to the data analysis. This work is part of the Shell-NWO/FOM-initiative Computational sciences for energy research of Shell and Chemical Sciences, Earth and Live Sciences, Physical Sciences, FOM and STW and an STW VIDI grant (No. 14868). This work was carried out on the national e-infrastructure of SURFsara, a subsidiary of SURF cooperation, the collaborative ICT organization for Dutch education and research.

References

[1] F. Porté-Agel, M. Bastankhah, and S. Shamsoddin. Wind-turbine and wind-farm flows: A review. *Boundary-Layer Meteorol.*, 74:1–59, 2020.
[2] R. J. A. M. Stevens and C. Meneveau. Flow structure and turbulence in wind farms. *Annu. Rev. Fluid Mech.*, 49:311–339, 2017.
[3] D. Medici, S. Ivanell, J.-Å Dahlberg, and P. H. Alfredsson. The upstream flow of a wind turbine: blockage effect. *Wind Energy*, 14(5):691–697, 2011.
[4] J. Bleeg, M. Purcell, R. Ruisi, and E. Traiger. Wind farm blockage and the consequences of neglecting its impact on energy production. *Energies*, 11(6):1609, 2018.
[5] A. R. Meyer Forsting and N. Troldborg. The effect of blockage on power production for laterally aligned wind turbines. *J. Phys. Conf. Ser.*, 625(1):012029, 2015.
[6] A. R. Meyer Forsting, N. Troldborg, and M. Gaunaa. The flow upstream of a row of aligned wind turbine rotors and its effect on power production. *Wind Energy*, 20(1):63–77, 2017.
[7] S. McTavish, D. Feszty, and F. Nitzsche. A study of the performance benefits of closely-spaced lateral wind farm configurations. *Renewable Energy*, 59:128–135, 2013.
[8] S. McTavish, S. Rodrigue, D. Feszty, and F. Nitzsche. An investigation of in-field blockage effects in closely spaced lateral wind farm configurations. *Wind Energy*, 18:1989–2011, 2015.
[9] A. Segalini and J.-Å Dahlberg. Blockage effects in wind farms. *Wind Energy*, 23(2):120–128, 2020.
[10] K. L. Wu and F. Porté-Agel. Flow adjustment inside and around large finite-size wind farms. *Energies*, 10(12):2164, 2017.
[11] E. Bou-Zeid, C. Meneveau, and M. B. Parlange. A scale-dependent Lagrangian dynamic model for large eddy simulation of complex turbulent flows. *Phys. Fluids*, 17:025105, 2005.
[12] C.-H. Moeng. A large-eddy simulation model for the study of planetary boundary-layer turbulence. *J. Atmos. Sci.*, 41:2052–2062, 1984.
[13] World Meterological Organization. *Guide to Meteorological Instruments and Methods of Observation, seventh edition*. World Meteorological Organization (WMO), Geneva, 2008.
[14] R. J. A. M. Stevens, J. Graham, and C. Meneveau. A concurrent precursor inflow method for large eddy simulations and applications to finite length wind farms. *Renewable Energy*, 68:46–50, 2014.
[15] M. Calaf, C. Meneveau, and J. Meyers. Large eddy simulations of fully developed wind-turbine array boundary layers. *Phys. Fluids*, 22:015110, 2010.
[16] A. Jimenez, A. Crespo, E. Migoya, and J. Garcia. Advances in large-eddy simulation of a wind turbine wake. *J. Phys. Conf. Ser.*, 75:012041, 2007.
[17] J. Meyers and C. Meneveau. Large eddy simulations of large wind-turbine arrays in the atmospheric boundary layer. *48th AIAA Aerospace Sciences Meeting Including the New Horizons Forum and Aerospace Exposition AIAA 2010-827 4 - 7 January 2010, Orlando, Florida*, pages AIAA 2010–827, 2010.
[18] T. Burton, D. Sharpe, N. Jenkins, and E. Bossanyi. *Wind Energy Handbook*. John Wiley & Sons, New York, 2001.
[19] F. Porté-Agel, Y.-T. Wu, and C. H. Chen. A numerical study of the effects of wind direction on turbine wakes and power losses in a large wind farm. *Energies*, 6:5297–5313, 2013.